acrt AI, Computer Science and Robotics Technology

IntechOpen Journals

SHORT COMMUNICATION

# Energy-Harvesting Device Based on Lead-Free Perovskite

J. A. Ajani Lakmini Jayarathna[1] and Kushal Ruthvik Kaja[2,*]

1 School of Integrated Science and Innovation, Sirindhorn International Institute of Technology, Thammasat University, Pathum Thani, Thailand
2 Department of Physics, Vellore Institute of Technology, Vijayawada, India
*Corresponding author. E-mail: ruthvikkushalk@gmail.com

*Citation*
J. A. Ajani Lakmini Jayarathna and Kushal Ruthvik Kaja (2024), Energy-Harvesting Device Based on Lead-Free Perovskite. *AI, Computer Science and Robotics Technology* 3(1), 1–9.

*DOI*
https://doi.org/10.5772/acrt.20240036



*Received*: 10 May 2024
*Accepted*: 21 August 2024
*Published*: 2 September 2024

## Abstract

This research investigates the solid-state synthesis of lead-free $(K, Na)_{0.5}NbO_3$ ceramics to improve the performance of triboelectric nanogenerators (TENGs) for energy-harvesting applications. The TENGs have developed as potential devices for converting mechanical energy into electrical energy. However, traditional TENG materials frequently include lead, which raises environmental and health problems. To overcome this issue, lead-free ceramics were examined as alternative materials with superior properties. In this work, a TENG was fabricated using potassium sodium niobate (KNN) ceramics as one triboelectric layer, Kapton as the other triboelectric layer, and a flexible substrate. The aim was to create TENGs with improved performance and environmental sustainability. The output performance of the TENG was estimated to be 70 V and 1100 nA. The TENG was further used to charge capacitors, light up an LED, and harvest energy from various body motions.

*Keywords:* lead-free, triboelectric, biomechanical, LED

## 1. Introduction

A triboelectric nanogenerator (TENG) converts mechanical energy into electrical energy using the triboelectric effect and electrostatic induction [1–3]. This unique device uses friction between two material combinations to generate an electric charge. TENGs may generate power from mechanical actions as simple as tapping, rubbing, or pushing, making them ideal for harvesting energy from ordinary activities or environmental sources such as wind or water [4–7]. TENGs have promising applications in wearable electronics, self-powered sensors, and renewable energy harvesting, providing a sustainable and efficient method of producing electricity without relying on existing power sources [8–12].

A lead-free piezoelectric material such as potassium sodium niobate (KNN) is gaining importance in energy harvesting and electronics due to its unique properties and environmental friendliness [13–16]. KNN exhibits a perovskite structure ($ABO_3$), where larger A-site cations (potassium and sodium) occupy the corners, smaller B-site cations (niobium and titanium) reside in the center, and oxygen anions position at the face centers, facilitating ferroelectric properties [17]. This configuration generates a highly ordered lattice that gives the KNN its piezoelectric potential. In addition, the crystal structure can be modified by doping or alloying to improve piezoelectric performance and stability, making it suitable for several applications [18, 19].

Unlike typical piezoelectric materials, which often contain harmful substances such as lead, KNN provides safer alternatives without compromising its effectiveness [20, 21]. This makes it an ideal solution for applications that require the extraction of energy from mechanical vibrations, movements, or deformations. KNN-based materials have been effectively incorporated into TENGs. When paired with triboelectric materials, KNN can greatly improve the energy conversion efficiency of TENGs. Previously, KNN-based materials have been explored commonly in the piezo–tribo electric hybrid energy device or single piezoelectric nanogenerator (PENG) by some authors to design various self-powered applications. Abdulla *et al.* have demonstrated a KNN/PVDF/MWCNT hybrid device based on composite films that can produce an output of 54.1 V and 29.4 μA [22]. Nair *et al.* have produced 2.1 V and 42 nA by simply tapping their fingers on a PENG device based on PVDF–KNN composites [23]. Verma *et al.* have used a PENG device based on KNN/PVDF composites for harvesting energy using body motions and generated a voltage of 11.2 V [24]. Composites based on PDMS–KNN–$x$BTO were prepared by Vivekananthan *et al.* to showcase a battery-free security system [19].

In the present work, a lead-free material KNN is synthesized, and various types of material characterization are performed. Furthermore, a TENG device was fabricated and operated in the vertical contact separation mode. The long-term stability output and glowing of LED were performed using TENG. It was used to harvest energy from various body motions. This innovative technology harnesses human motion to potentially power wearable devices or consumer electronics, offering a sustainable energy source.

## 2. Synthesis and experimental techniques

The typical solid-state reaction approach can produce KNN powder. Initially, high-purity oxides and carbonates such as potassium carbonate ($K_2CO_3$), sodium carbonate ($Na_2CO_3$), and niobium pentoxide ($Nb_2O_5$), procured from Loba Chemie, India, were taken in appropriate equimolar amounts. The ingredients were uniformly mixed in an agate mortar by adding alcohol as a medium for the following two hours to achieve a homogeneous mixture and then dried to collect the powder mixture. This homogeneous mixture was then transferred into an alumina crucible and put into a muffle furnace at 900 °C for 5 h to obtain the crystalline phase. After calcination, the powder was collected for various types of characterization. The TENG device is fabricated by taking PET as a substrate, and copper tape is used as an electrode. The calcinated KNN powder is spread on the copper electrode and fixed by cold press, which was used as a positive triboelectric layer and Kapton is taken as another triboelectric layer. The device is neither packed nor polled; hence the contribution of piezoelectric behavior of KNN is negligible. Therefore, this design setup can only act as a triboelectric nanogenerator. The dielectric properties were measured by using a pellet. For this purpose, a pelletizer was used to cold-press the KNN powder in disc shape (dimension 10 mm and thickness 1.5 mm) with the help of an organic binder, namely polyvinyl alcohol 2 wt%.

The X-ray diffractometer (XRD; Rigaku, Japan), with Cu–Kα radiation operating at ambient temperature and the X-ray source wavelength $\lambda = 1.5406$ Å, was utilized to measure the X-ray spectra. Using a 514 nm excitation source, a Raman spectrometer (LabRAM, Japan) was used to record the Raman spectrum analysis of KNN particles. Using a scanning electron microscope (SEM; Zeiss Sigma 300, USA), the surface morphology of KNN particles was investigated. The dielectric properties were measured using an impedance analyzer (Hioki IM3470, Japan) at room temperature. The TENG output was measured and traced using a Keithley 6514 electrometer and a linear motor was used to apply periodic contact separation of TENG.

## 3. Results and discussion

The KNN ceramics are synthesized by solid-state reaction. Figure 1a shows the Rietveld analysis of XRD spectra of KNN at room temperature. The KNN ceramics are seen to have an orthorhombic symmetry [25–27]. Using the MAUD (Materials Analysis Using Diffraction) tool, a Rietveld refinement of the XRD patterns is conducted to establish the crystal lattice parameters [28]. The crystal lattice parameters are as follows: $a = 3.9459$ Å, $b = 5.6447$ Å, and $c = 5.6764$ Å. The Raman spectra of KNN powders at room temperature are displayed in Figure 1b. There are three characteristic Raman peaks (870 $cm^{-1}$, 620 $cm^{-1}$, and 250 $cm^{-1}$) in the spectra

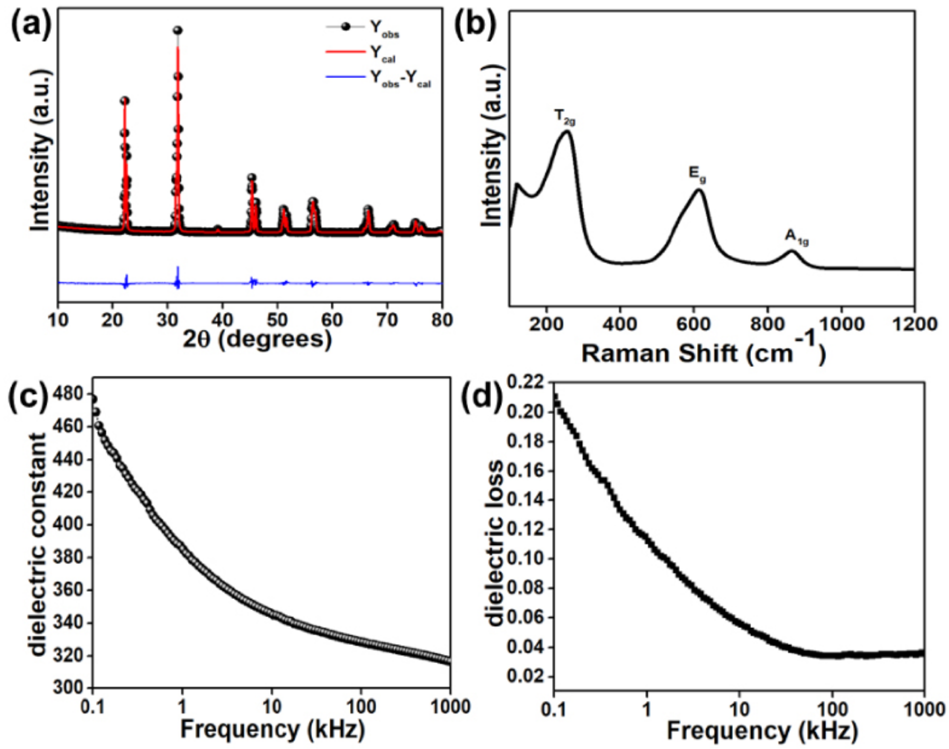


*Figure 1.* (a) Rietveld refinement of XRD pattern of KNN ceramics, (b) Raman spectra of KNN ceramics, and (c, d) dielectric constant and loss of KNN ceramics at room temperature, respectively.

of KNN, which are related to the internal vibrations of the $NbO_6$ octahedron. Other groups also reported similar Raman spectra of KNN ceramics [17, 29, 30]. The dielectric constant and loss of KNN ceramics at room temperature are measured and presented in Figures 1(c,d), respectively. It shows that both dielectric constant and loss are higher at low frequencies and reduced at higher frequency zones. The dielectric constant is higher at low frequencies due to the reason that all polarizations are activated in this zone, and as one moves to a higher frequency, the dipoles cannot follow the fast-changing electric field leading to a decrease in the dielectric constant value [31, 32]. Compared to the grain borders, the grains are far more conducting. Only at low frequencies does the movement of charge carriers to the grain border, which causes a greater energy loss, predominates. Because of this, the loss factor in this low-frequency region is higher than that in the high-frequency region [33].

Figure 2a displays the SEM micrograph of the KNN sample. The surface morphology displays the densely packed and cube-shaped grains. Figure 2b shows the color mapping of the elements present in KNN ceramics such as K, Na, Nb, and O, which spread uniformly over the surface. Figure 2c shows the EDS spectra of

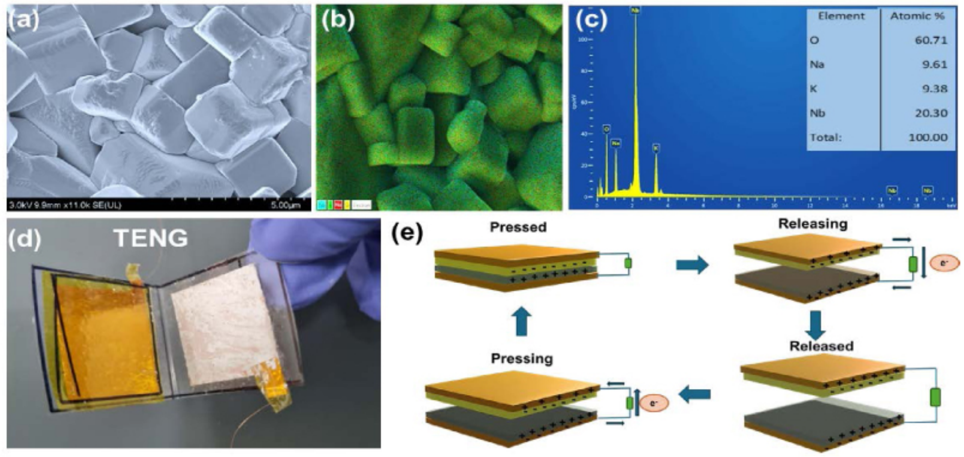


*Figure 2.* (a) SEM micrograph of KNN ceramics, (b) color mapping of elements K, Na, and Nb in KNN ceramics, (c) EDS spectra with atomic percentage present in KNN ceramics, (d) digital picture of TENG KNN powder and Kapton as triboelectric layers, and (e) working mechanism of TENG operation in vertical contact separation mode.

KNN ceramics and atomic percentage in the insert. Figure 2d shows a digital image of the fabricated TENG using KNN powder, with Kapton serving as the triboelectric layer. The device is tested by vertical contact and separation mode. Due to contact, electrification charges are generated on the surfaces of triboelectric layers. As a result, negative charges are developed on Kapton whereas positive charges are formed on another triboelectric layer (KNN powders). Here, Kapton acts as a negative triboelectric layer. The detailed working mechanism of the TENG is shown in Figure 2e.

Figure 3a shows the voltage and Figure 3b the current of the TENG, which has an active area of 2. 5 cm × 2. 5 cm. Figure 3c shows the long-term stability of the TENG device, confirming the device is useful for many applications. The stability was measured at a constant force of 5 N and 2 Hz. Figure 3d shows the charging of capacitors using TENG. The output of TENG is AC, which is converted to DC using a bridge rectifier. Figure 3e shows the powering of an LED using TENG. Here the digital image of the LED in off and on conditions is shown. Hence it can be confirmed that the TENG can act as a sustainable power source. Figures 4a–f show the voltage of the TENG attached to various body parts. The TENG can be activated by performing actions like walking, tapping, and stretching, which transforms mechanical energy into electrical power. Thus, TENG provides a sustainable energy source by using human motion to power wearables, sensors, and small electronics.

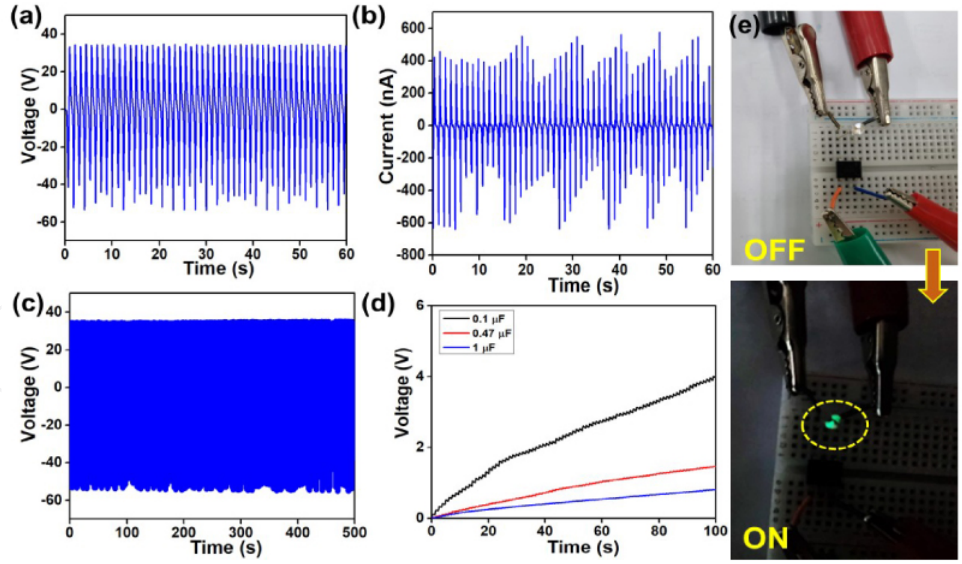


*Figure 3.* (a) Voltage, (b) current, (c) stability of TENG voltage, (d) charging of capacitor using TENG, and (e) digital image of LED glowing using TENG.

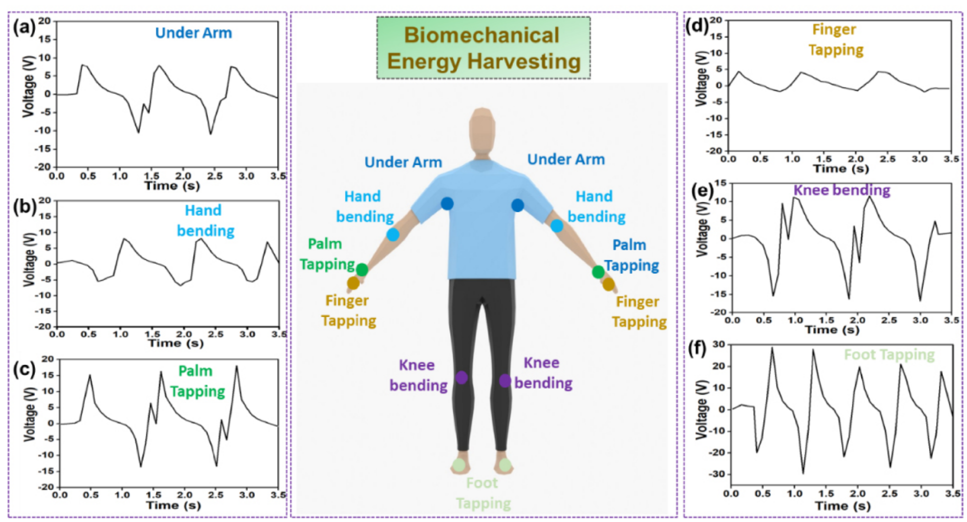


*Figure 4.* (a–f) Biomechanical energy harvesting using various human activities and corresponding voltage of TENG output.

## 4. Conclusions

This study explores the synthesis of lead-free $(K, Na)_{0.5}NbO_3$ ceramics via the solid-state method. Various types of material characterization such as structural, morphology, and electrical properties of KNN are provided in detail. TENGs follow the principle of contact electrification and electrostatic induction. Lead-free ceramics have been investigated as viable alternatives to lead-based ceramics. In this research, a TENG operating in vertical contact separation mode was constructed utilizing one triboelectric layer composed of KNN ceramics, another layer consisting of Kapton, and a PET flexible substrate. Experimental results showcased the output performance of TENG reaching 70 V and 1100 nA. Furthermore, the TENG was employed to charge capacitors, illuminate LEDs, and harness energy from diverse bodies. This work focuses on efficient and environmentally friendly, energy-harvesting devices for a wide range of applications such as wearable electronics and self-powered sensors.

## Acknowledgement

ALJ gratefully acknowledges the prestigious Faculty's Quota Scholarship awarded by Sirindhorn International Institute of Technology, Thammasat University, Thailand.

## Conflict of interest

The authors declare no conflict of interest.

## References

1 Panda S, Hajra S, Oh Y, Oh W, Lee J, Shin H, et al. Hybrid nanogenerators for ocean energy harvesting: mechanisms, designs, and applications. *Small*. 2023;**19**: 2300847.

2 Elsanadidy E, Mosa IM, Luo D, Xiao X, Chen J, Wang ZL, et al. Advances in triboelectric nanogenerators for self-powered neuromodulation. *Adv Funct Mater*. 2023;**33**: 2211177.

3 Babu A, Bochu L, Potu S, Kaja R, Madathil N, Velpula M, et al. Facile direct growth of ZIF-67 metalorganic framework for triboelectric nanogenerators and their application in the internet of vehicles. *ACS Sustain Chem Eng*. 2023;**11**: 16806–16817.

4 Yong S, Wang J, Yang L, Wang H, Luo H, Liao R, et al. Auto-switching self-powered system for efficient broad-band wind energy harvesting based on dual-rotation shaft triboelectric nanogenerator. *Adv Energy Mater*. 2021;**11**: 2101194.

5 Khwanming R, Pongampai S, Vittayakorn N, Charoonsuk T. Cellulose-based fabrics triboelectric nanogenerator: Effect of fabric microstructure on its electrical output. *J Metals Mater Miner*. 2023;**33**: 1673.

6 Sriphan S, Vittayakorn N. Facile roughness fabrications and their roughness effects on electrical outputs of the triboelectric nanogenerator. *Smart Mater Struct*. 2018;**27**: 105026.

7 Ruthvik K, Babu A, Supraja P, Navaneeth M, Mahesh V, Uday Kumar K, et al. High-performance triboelectric nanogenerator based on 2D graphitic carbon nitride for self-powered electronic devices. *Mater Lett*. 2023;**350**: 134947.

8 Hajra S, Panda S, Song S, Panigrahi BK, Pakawanit P, Jeong SM, et al. Flexible composite material for self-powered applications via triboelectricity and mechanoluminescence: PDMS/ZnS:Cu composites. *Nano Energy*. 2023;**114**: 108668.

9 Divya S, Hajra S, Panda S, Vivekananthan V, Mistewicz K, Joon Kim H, et al. A review on the next generation of healing: Exploring the use of triboelectric nanogenerators in wound care. *Chem Phys Lett*. 2023;**826**: 140648.

10 Divya S, Panda S, Hajra S, Jeyaraj R, Paul A, Park SH, et al. Smart data processing for energy harvesting systems using artificial intelligence. *Nano Energy*. 2023;**106**: 108084.

11 Sathya Prasanna AP, Vivekananthan V, Khandelwal G, Alluri NR, Maria Joseph Raj NP, Anithkumar M, et al. Green energy from edible materials: triboelectrification-enabled sustainable self-powered human joint movement monitoring. *ACS Sustain Chem Eng*. 2022;**10**: 6549–6558.

12 Jiang D, Lian M, Xu M, Sun Q, Xu BB, Thabet HK, et al. Advances in triboelectric nanogenerator technology—applications in self-powered sensors, Internet of things, biomedicine, and blue energy. *Adv Compos Hybrid Mater*. 2023;**6**: 57.

13 Sivaprakash P, Divya S, Esakki Muthu S, Ali A, Jaglicic Z, Hwan Oh T, et al. Effect of rare earth Europium (Eu3+) on structural, morphological, magnetic and dielectric properties of $NiFe2O_4$ nanoferrites. *Mater Sci Eng B*. 2024;**301**: 117200.

14 Behera SA, Hajra S, Panda S, Amanat A, Achary PGR. Structural and electrical properties of 0.98($KO_{0.5}NaO_{0.5}NbOO_3$)-0.02($BiO_{0.5}NaO_{0.5}TiOO_3$) ceramics. *J Metals Mater Miner*. 2023;**33**: 1894.

15 Rajput S, Keshri S. Effect of A-site modification on structural and microwave dielectric properties of calcium titanate. *J Metals Mater Miner*. 2022;**32**: 118–125.

16 Kumar N, Mahale B, Muzata TS, Ranjan R. Energy harvesting with flexible piezocomposite fabricated from a biodegradable polymer. *Int J Energy Res*. 2021;**45**: 19395–19404.

17 Mahesh P, Pamu D. Raman and dielectric studies on lead free ($K_{0.5}Na_{0.5}$) $NbO_3$ piezoelectric ceramics. *IOP Conf Ser: Mater Sci Eng*. 2015;**73**: 012141.

18 Li Y-M, Shen Z-Y, Wu F, Pan T-Z, Wang Z-M, Xiao Z-G. Enhancement of piezoelectric properties and temperature stability by forming an MPB in KNN-based lead-free ceramics. *J Mater Sci: Mater Electron*. 2014;**25**: 1028–1032.

19 Vivekananthan V, Alluri NR, Chandrasekhar A, Purusothaman Y, Gupta A, Kim S-J. Zero-power consuming intruder identification system by enhanced piezoelectricity of $K_{0.5}Na_{0.5}NbO_3$ using substitutional doping of BTO NPs. *J Mater Chem C*. 2019;**7**: 7563–7571.

20 Zhang D-Q, Wang D-W, Zhu H-B, Yang X-Y, Lu R, Wen B, et al. Synthesis and characterization of single-crystalline (K,Na)$NbO_3$ nanorods. *Ceram Int*. 2013;**39**: 5931–5935.

21 Egerton L, Dillon DM. Piezoelectric and dielectric properties of ceramics in the system potassium–sodium niobate. *J Am Ceram Soc*. 1959;**42**: 438–442.

22 Abdullah AM, Sadaf MUK, Tasnim F, Vasquez H, Lozano K, Uddin MJ. KNN based piezo-triboelectric lead-free hybrid energy films. *Nano Energy*. 2021;**86**: 106133.

23 Nair KS, Varghese H, Chandran A, Hareesh UNS, Chouprik A, Spiridonov M, et al. Synthesis of KNN nanoblocks through surfactant-assisted hot injection method and fabrication of flexible piezoelectric nanogenerator based on KNN-PVDF nanocomposite. *Mater Today Commun*. 2022;**31**: 103291.

24 Verma K, Sharma R. A flexible piezoelectric generator based on KNN/PVDF composite films: role of KNN concentration on the piezoelectric performance of generator. *Chin J Phys*. 2023;**84**: 198–215.

25 Chang Y, Yang Z, Chao X, Zhang R, Li X. Dielectric and piezoelectric properties of alkaline-earth titanate doped ($K_{0.5}Na_{0.5}$)$NbO_3$ ceramics. *Mater Lett*. 2007;**61**: 785–789.

26 He Y, Wang Z, Hu X, Cai Y, Li L, Gao Y, et al. Orientation-dependent piezoresponse and high-performance energy harvesting of lead-free (K,Na) $NbO_3$ nanorod arrays. *RSC Adv*. 2017;**7**: 16908–16915.

27 Nandini R, Krishna M, Suresh A, Rao KN. Effect of calcination kinetics and microwave sintering parameters on dielectric and pieizo-electric properties of ($K_{0.5}Na_{0.5}$)$NbO_3$ ceramics. *Iran J Mater Sci Eng*. 2018;**15**: 14–31.

28 Daniel CS, Zeng X, Michalik Š, Hunt SA, da Fonseca JQ. Application of a new method for accurate determination of and texture in Ti-6Al-4V from synchrotron diffraction intensities. *Mater Charact*. 2023;**199**: 112769.

29 Połomska M, Hilczer B, Kosec M, Malič B. Raman Scattering Studies of Lead Free $(1-x)K_{0.5}Na_{0.5}NbO_{3}-xSrTiO_3$ relaxors. *Ferroelectrics*. 2008;**369**: 149–156.

30 Trodahl H, Klein N, Damjanovic D, Setter N, Ludbrook B, Rytz D, et al. Raman spectroscopy of $(K,Na)NbO_3$ and $(K,Na)_{1-x}Li_xNbO_3$. *Appl Phys Lett*. 2008;**93**: 262901.

31 Barik SK, Gogoi KK, Sahoo S, Kim HJ, Hajra S. A lead-free perovskite $Bi_{1/2}(Na_{1/4}Li_{1/4})TiO_3$: investigation on structural, electrical properties, and device application. *J Mater Sci: Mater Electron*. 2021;**32**: 4629–4638.

32 Gupta P, Mahapatra PK, Choudhary RNP. Structural and electrical characteristics of rare-earth modified bismuth layer structured compounds. *J Alloys Compd*. 2021;**863**: 158457.

33 Gupta P, Padhee R, Mahapatra PK, Choudhary RNP. Structural, dielectric, impedance and modulus spectroscopy of $Bi_2NdTiVO_9$ ferroelectric ceramics. *J Mater Sci: Mater Electron*. 2017;**28**: 17344–17353.